Carrier Lifetimes in Silicon

Dieter K. Schroder, *Fellow, IEEE*

***Abstract*—Carrier lifetimes in semiconductors are being rediscovered by the Si IC community, because the lifetime is a very effective parameter to characterize the purity of a material or device. It has become a process and equipment characterization parameter. The various recombination mechanisms are discussed and the concept of recombination and generation lifetime is presented. We show that surface recombination/generation plays an important role in today's high purity Si and will become yet more important as bulk impurity densities in Si are reduced further. Furthermore, the dependence of lifetime on impurity energy level and minority carrier injection level is discussed. Concepts are stressed in the paper, with the necessary equations to clarify these concepts. Wherever possible, the concepts are augmented with experimental data, with particular emphasis on the case of iron in silicon, because Fe is one of the most important impurities in Si today. We have used Si in the examples because lifetime measurements are most commonly made in Si.**

I. Introduction

THE TOPIC of carrier lifetime in semiconductors is almost as old as semiconductors themselves. The basic theory of electron-hole pair (ehp) recombination through recombination centers (sometimes called traps) was put forth in 1952 in the well known and frequently quoted papers by Hall [1] and Shockley and Read [2]. Hall later expanded on his original brief letter [3]. Many papers have been published since then dealing with lifetime and the basic recombination mechanisms are well known for many semiconductors. Why do we need another paper on this topic? There is obviously nothing really new; yet lifetimes, their measurement, and measurement interpretation are frequently misunderstood even today. Furthermore, this is a propitious time, since the measurement of lifetimes, at least in Si, is undergoing a renaissance. Lifetimes and diffusion lengths are measured more frequently today in the IC industry than they have been for many years.

Lifetime is one of very few parameters giving information about the low defect densities consistent with today's IC's. What other technique can detect defect densities as low as 10^{10}–10^{11} cm^{-3} in a simple room temperature measurement? Further, the availability of commercial equipment makes these measurements relatively simple. It is for these reasons that the IC community, largely concerned with unipolar MOS devices in which lifetime plays a minor role, has adopted lifetime measurements as a "process cleanliness monitor." However, to have faith in the measurements, it is necessary to understand the measured entity. For example, since today's Si has few deep level impurities, surfaces play an increasingly important role during lifetime measurements. We have tried, in this paper, to put together the most important aspects of "lifetime". What types of lifetimes are there, how do they depend on material and device parameters like energy level in the bandgap, injection level, and surfaces, for example? How is lifetime measured and what does the measurement represent?

Carrier lifetime is frequently misused in semiconductor technology, although the concept of a lifetime seems simple enough. Unfortunately, problems arise with the realization that different measurement methods give widely differing values for the same material or device structure. In most cases, the reasons for these discrepancies are fundamental and are not due to a deficiency of the measurement. The difficulty with defining a lifetime is that we are describing a property of a carrier within the semiconductor rather than the property of the semiconductor itself. Although we usually quote a single numerical value, we are measuring some weighted average of the behavior of carriers influenced by surfaces, interfaces, doping barriers, the density of carriers besides the properties of the semiconductor material and its temperature. The issue is further complicated by the term *lifetime* to refer to both *recombination lifetime* and *generation lifetime*. It is, of course, understood that the minority carrier diffusion length is related to the lifetime and is an equally valid parameter to characterize a device or material.

Lifetimes fall into two primary categories: *recombination lifetimes*; and *generation lifetimes* [4]. The concept of recombination lifetime τ_r holds when excess carriers decay as a result of recombination. Generation lifetime τ_g applies when there is a paucity of carriers, as in the space-charge region (scr) of a reverse-biased diode or MOS device and the device tries to attain equilibrium. During recombination an electron-hole pair ceases to exist on average after a time τ_r, illustrated in Fig. 1(a). The generation lifetime, by analogy, is the time that it takes on average to generate an ehp, illustrated in Fig. 1(b).

When these recombination and generation events occur in the bulk, they are characterized by τ_r and τ_g. When they occur at the surface, they are characterized by the *surface recombination velocity* s_r and the *surface generation velocity* s_g, also illustrated in Fig. 1. Since devices consist of bulk regions and surfaces, both bulk and surface recombination or generation occur simultaneously and their separation is sometimes quite difficult. Some methods allow this separation while others do not. The measured lifetimes are always *effective* lifetimes consisting of bulk and surface components. We do not address lifetime measurement techniques here. They are covered elsewhere [5].

Manuscript received December 27, 1995; revised June 25, 1996. The review of this paper was arranged by Editor P. N. Panayotatos. This work was supported in part by Sematech and the Silicon Supply companies (Komatsu Electronic Metals, MEMC Electronic Materials, SEH America, Mitsubishi Silicon America, Sumitomo Sitix Silicon, and Wacker Siltronic Corp.) through the Center for Defect-Free Wafer Science and Technology.

The author is with the Department of Electrical Engineering and the Center for Solid State Electronics Research, Arizona State University, Tempe AZ 85287-5706 USA.

Publisher Item Identifier S 0018-9383(97)00319-5.

0018–9383/97$10.00 © 1997 IEEE

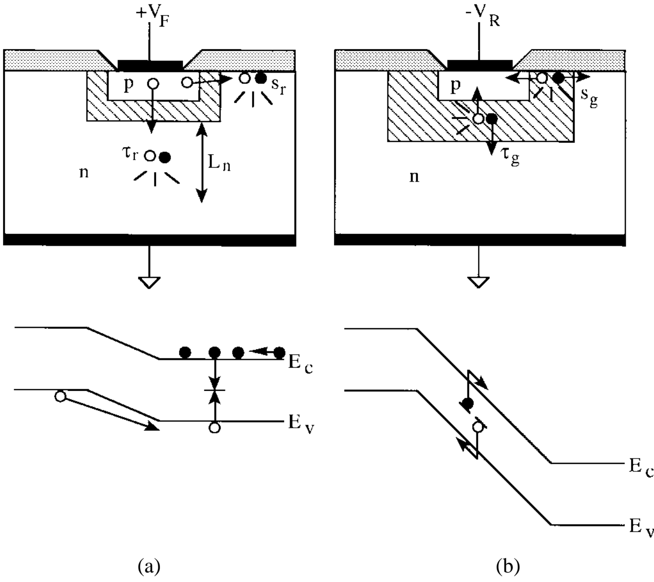

Fig. 1. (a) Forward-biased and (b) reverse-biased junction.

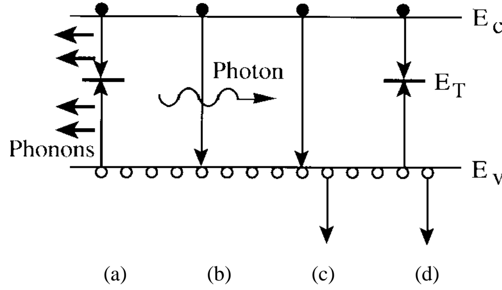

Fig. 2. Recombination mechanisms: (a) SRH, (b) radiative, (c) direct Auger, and (d) trap-assisted Auger.

II. Recombination Lifetime

The recombination rate depends nonlinearly on the departure of the carrier densities from their equilibrium values. We consider a p-type semiconductor and are chiefly concerned with the behavior of the minority electrons. For a semiconductor device containing a pn junction we are concerned with the quasineutral regions when discussing recombination and the space-charge region when discussing generation. Three main recombination mechanisms determine the recombination lifetime: 1) *Shockley–Read–Hall* or *multiphonon* recombination characterized by the lifetime $\tau_{\rm SRH}$; 2) *radiative* recombination characterized by $\tau_{\rm rad}$; and 3) *Auger* recombination characterized by $\tau_{\rm Auger}$. These three recombination mechanisms are illustrated in Fig. 2. The recombination lifetime τ_r is determined by the three mechanisms according to the relationship [5]

$$\tau_r = \frac{1}{\tau_{\rm SRH}^{-1} + \tau_{\rm rad}^{-1} + \tau_{\rm Auger}^{-1}}. \tag{1}$$

During SRH recombination, electron-hole pairs recombine through deep-level impurities, characterized by the impurity density N_T, energy level E_T in the bandgap, and capture cross sections σ_n and σ_p for electrons and holes, respectively. The energy liberated during the recombination event is dissipated by lattice vibrations or phonons, illustrated in Fig. 2(a). The SRH lifetime is given by [2]

$$\tau_{\rm SRH} = \frac{\tau_p(n_o + n_1 + \Delta n) + \tau_n(p_o + p_1 + \Delta p)}{p_o + n_o + \Delta n} \tag{2}$$

where p_o and n_o are the equilibrium hole and electron densities, Δn and Δp are the excess carrier densities taken to be equal in the absence of trapping, and n_1, p_1, τ_n, and τ_p are defined as

$$n_1 = n_i e^{(E_T - E_i)kT}; \quad p_1 = n_i e^{-E_T - E_i)kT} \tag{3a}$$

$$\tau_p = \frac{1}{\sigma_p v_{\rm th} N_T}; \quad \tau_n = \frac{1}{\sigma_n v_{\rm th} N_T}. \tag{3b}$$

During radiative recombination ehps recombine directly from band to band with the energy carried away by photons shown in Fig. 2(b). The radiative lifetime is [5]

$$\tau_{\rm rad} = \frac{1}{B(p_o + n_o + \Delta n)}. \tag{4}$$

B is usually termed the radiative recombination coefficient. We include in B both the radiative recombination coefficient B_r and the trap-assisted Auger coefficient B_T, with $B = B_{\rm rad} + B_T$. Even though trap-assisted Auger recombination, shown in Fig. 2(d), is not a radiative event, we include it here because it has the same carrier density dependence as radiative recombination. For Si, $B_{\rm rad} = 2\times10^{-15}$ cm^3/s and B_T ranges from 1×10^{-15} to 9×10^{-15} cm^3/s [6]. The radiative lifetime is inversely proportional to the carrier density because in band-to-band processes both electrons and holes must be present simultaneously for a recombination event to take place.

During Auger recombination, illustrated in Fig. 2(c), the recombination energy is absorbed by a third carrier. Because three carriers are involved in the recombination event, the Auger lifetime is inversely proportional to the carrier density squared. For a p-type semiconductor, the Auger lifetime is given by [5]

$$\tau_{\rm Auger} = \frac{1}{C_p(p_o^2 + 2p_o\Delta n + \Delta n^2)} \tag{5}$$

where C_p is the Auger recombination coefficient.

The recombination lifetime according to (1) is plotted in Fig. 3. At high carrier densities, the lifetime in Si is controlled by Auger recombination and at low densities by multiphonon recombination. Radiative recombination plays almost no role in Si, but is important in direct bandgap semiconductors like GaAs. The Auger lifetime appears to be described by more than one Auger coefficient. The data of Fig. 3 can be reasonably well fitted with $C_p = 1.1 \times 10^{-30}$ cm^6/s or $C_p = 10^{-31}$ cm^6/s. The reason for this discrepancy is not clear.

When do these three lifetimes apply? SRH recombination takes place whenever there are impurities or defects in the semiconductor. Since semiconductors always contain some impurities, this mechanism is always active. It is particularly important for indirect bandgap semiconductors. The SRH lifetime depends inversely on the density of recombination centers and capture cross sections but does not depend directly on the energy level of the impurity. It does depend indirectly

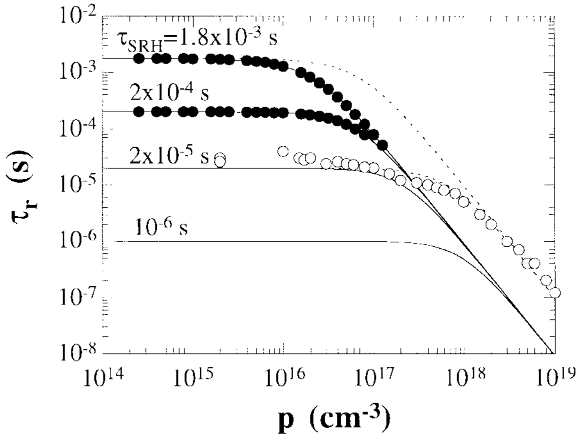

Fig. 3. Recombination lifetime τ_r versus majority carrier density for p-type Si; $B = 1.3 \times 10^{-14}$ cm^3/s; $C_p = 1.1 \times 10^{-30}$ cm^6/s (solid lines), $C_p = 10^{-31}$ cm^6/s (dashed line). Data from [5] and [6].

on the energy level, because the capture cross section tends to be highest for impurities with E_T near the center of the bandgap and lowest for E_T near the conduction or valence band. Band-to-band SRH recombination is very unlikely in Si.

Radiative recombination is important in direct bandgap materials like GaAs and InP, where the conduction band minimum lies at the same crystal momentum value as the valence band maximum. During the recombination event, phonons are not required, since the energy is dissipated by photons. Radiative recombination is relatively unimportant in Si, because its radiative lifetime is extremely high.

Auger recombination is typically observed in both direct and indirect bandgap semiconductors when either the doping density or the excess carrier density is very high. Similar to the radiative lifetime, the Auger lifetime is independent of any impurity density. Auger recombination is the ultimate recombination mechanism for devices operating at very high injection or at very high doping densities. It is also the dominant recombination mechanism for narrow bandgap semiconductors (e.g., HgCdTe used for infrared detectors).

Both radiative and Auger recombination can also occur through intermediate energy levels. When ehps recombine radiatively through intermediate levels, photons are generally emitted for only one of the transitions. This recombination mechanism is used in light-emitting phosphors that are deliberately doped with impurities of a particular kind to generate light of a particular wavelength. A good example of this is the cathode ray tube used in color television receivers where excess carriers in phosphors bombarded by the electron beam emit red, blue or green light upon recombination.

A. Shockley–Read–Hall Recombination Lifetime

In this section we illustrate the effect of impurity energy level and carrier injection level on the SRH lifetime. The low-level lifetime $\tau_{\mathrm{SRH}}(ll)$ holds when the excess minority carrier density Δn is small compared to the equilibrium majority carrier density p_o, i.e., $\Delta n = \Delta p \ll p_o$. For high-level injection $\Delta n = \Delta p \gg p_o$. We assume here that $\Delta n = \Delta p$, valid when trapping can be neglected.

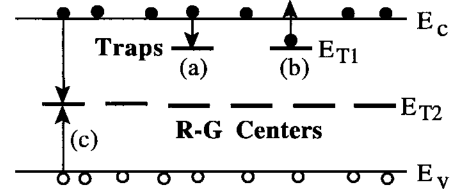

Fig. 4. (a) Capture, (b) emission form a trapping event, and (c) a recombination event.

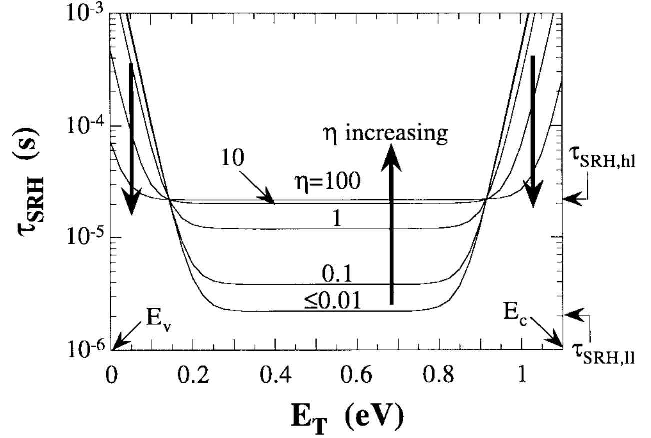

Fig. 5. τ_{SRH} versus E_T for $N_T = 10^{12}$ cm^{-3}, $p_o = 10^{16}$ cm^{-3}, $\sigma_n = 5 \times 10^{-14}$ cm^2, $\sigma_p = 5 \times 10^{-15}$ cm^2; the normalized injection level is $\eta = \Delta n/p_o$.

Trapping is the mechanism by which some of the excess ehps, originally created in equal densities, are trapped temporarily on impurities, as illustrated in Fig. 4. Those electrons captured on level E_{T1} [Event (a)] can be subsequently emitted back to the conduction band by thermal emission [Event (b)]. Alternately, they can be emitted optically by background light on the sample. As long as electrons are trapped, $\Delta n \neq \Delta p$. When trapping is an issue, lifetime measurements are frequently made in the presence of background illumination to reduce the effect. Trapping is of major concern in wide bandgap semiconductors, but is usually considered to be of minor concern in semiconductors like Si. Fig. 4 illustrates why the word “trap” is best not used when recombination or generation occurs; “recombination/generation (R–G) center” is better.

The SRH lifetime is given in (2). To see the effect of impurity energy level E_T and injection level on the lifetime, we plot τ_{SRH} versus E_T as a function of normalized injection level $\eta = \Delta n/p_o$ in Fig. 5. For low-level injection, according to (2), the low-level lifetime $\tau_{\mathrm{SRH}}(ll)$ becomes

$$\tau_{\mathrm{SRH}}(ll) \approx \tau_p(n_1/p_o) + \tau_n(1 + p_1/p_o) \qquad (6)$$

where $n_o \ll n_1$ and $n_o \ll p_o$. Equation (6) is sometimes further approximated as

$$\tau_{\mathrm{SRH}}(ll) \approx \tau_n. \qquad (7)$$

Equation (7) is only an approximation, however, as illustrated in Fig. 5 valid for $n_1 \ll p_o$ and $p_1 \ll p_o$. The central portion of the curve for $\eta \leq 0.01$ is $\tau_n(\eta = \Delta n/p_o)$. However, τ_{SRH} increases for impurities with energy levels

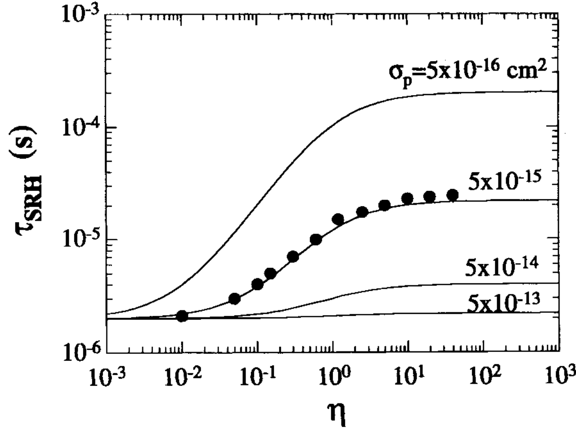

Fig. 6. τ_{SRH} versus η for $N_T = 10^{12}\mathrm{cm}^{-3}, p_o = 10^{16}$ cm$^{-3}, E_T = 0.4$ eV, $\sigma_n = 5 \times 10^{-14}$ cm$^2, \eta = \Delta n/p_o$; experimental data points adapted from [7].

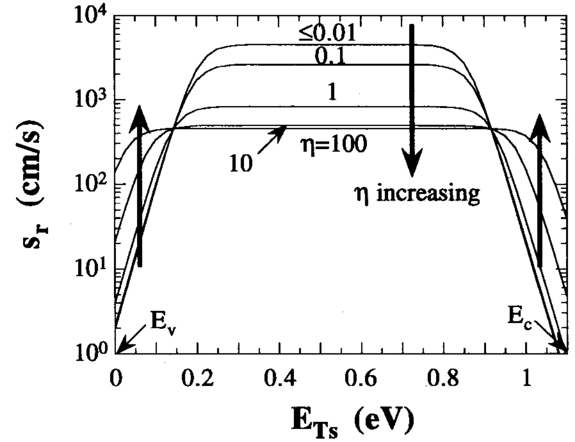

Fig. 7. s_r versus E_{Ts} for $N_{it} = 10^{10}$ cm$^{-3}, p_{os} = 10^{16}$ cm^{-3}, $\sigma_{ns} = 5 \times 10^{-14}$ cm$^2, s_{ps} = 5 \times 10^{-17}$ cm^2; the injection level is $\eta = \Delta n_s/p_{os}$.

toward the band edges even at low $\eta \cdot \tau_{\mathrm{SRH}}$ also depends on the excess carrier density, as illustrated in Fig. 5. If $\Delta n = \Delta p \gg p_o, n_o, p_1$ and n_1 (high level injection) then the lifetime becomes

$$\tau_{\mathrm{SRH}}(hl) \approx \tau_n + \tau_p. \tag{8}$$

Under conditions valid for (7) or (8), τ_{SRH} for a given energy level and for given capture cross sections always *increases* with injected carrier density, as illustrated in Fig. 6. However, as shown in Fig. 5, for n_1 or $p_1 \gg (\Delta n = \Delta p) \gg p_o, n_o$, the lifetime *decreases* with injection level. The dependence of τ_{SRH} on η is illustrated in Fig. 5 by the vertical arrows. This figure clearly shows that τ_{SRH} does not always increase with increasing injection level, as is often stated.

What are typical excess carrier densities during τ_r or minority carrier diffusion length measurements? That depends on the measurement technique. The injection level varies during photoconductance decay (PCD) measurements, as carrier density changes during the measurement. It is certainly possible to make PCD measurements at low injection levels. However, many PCD measurements are made under high injection levels. Sometimes this is done to reduce surface recombination, a point addressed later. During surface photovoltage (SPV) measurements, the open-circuit voltage is usually kept low compared to kT/q, typically a few mV, to ensure a linear relationship between surface photovoltage and excess carrier density. The excess carrier density is $\Delta n = n_o[\exp(qV/kT) - 1]$. Δn is proportional to V only if $V \ll kT/q$, since $n_o[\exp(qV/kT) - 1] \approx n_o qV/kT$ in that case. This corresponds to $\Delta n \ll p_o$, i.e., the device must clearly be in low-level injection. SPV measurements can be made under constant voltage or constant photon flux density conditions and the injection level may change with wavelength. Clearly, the injection level needs to be considered when comparing lifetimes determined by different techniques for the lifetimes can be very different as illustrated in Fig. 5.

B. Shockley–Read–Hall Surface Recombination Velocity

Besides SRH bulk recombination there is also SRH surface recombination at bare surfaces or interface recombination at insulator/semiconductor interfaces. Analogous to the SRH lifetime in (1), the SRH *surface recombination velocity* is given by [5]

$$s_r = \frac{s_n s_p(p_{os} + n_{os} + \Delta n_s)}{s_n(n_{os} + n_{1s} + \Delta n_s) + s_p(p_{os} + p_{1s} + \Delta p_s)} \tag{9}$$

where

$$s_n = \sigma_{ns} v_{\mathrm{th}} N_{it}; \quad s_p = \sigma_{ps} v_{\mathrm{th}} N_{it}. \tag{10}$$

The subscript "s" refers to the appropriate quantity at the surface, with carrier densities being in units of cm^{-3}. The interface trap density N_{it}, in units of cm^{-2}, is assumed constant in (9).

The surface state density and energy distribution of a bare surface are generally only poorly known. The interface trap density at the SiO_2/Si interface is quite well understood and controlled. Its energy, density, and capture cross sections vary throughout the bandgap. To treat such an interface correctly, requires an integration of the recombination generation rate expression. However, for a given measurement it is frequently only a small portion of the interface trap density that is active during recombination or generation for any given bias. Treating the interface trap density as approximately constant is a reasonable assumption. Including the full version only complicates the issue and does not add to the concepts addressed here. It is worth pointing out that the recombination statistics of the interface traps remain unchanged even when there is a distribution of them, since the spatial distance between the traps limits the interaction between them.

The dependence of s_r on injection level and energy level is shown in Fig. 7. Contrary to Fig. 5 where the lifetime increases or decreases with injection level, the surface recombination velocity exhibits the opposite behavior. Of course, both increased lifetime and reduced surface recombination velocity signify reduced recombination. The dependence of s_r on injection level and capture cross section is shown in Fig. 8. The theoretical curves in this figure were calculated with capture cross sections appropriate for interface traps at SiO_2/Si interfaces [8]. The capture cross sections in Fig. 7

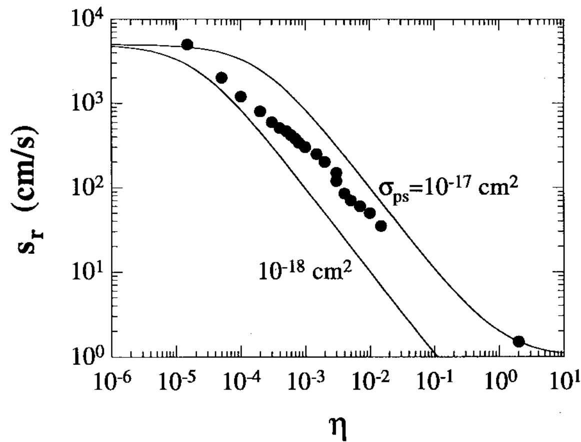

Fig. 8. s_r versus η as a function of σ_{ps} for $N_{it} = 10^{10}$ cm^{-2}, $p_{os} = 10^{16}$ cm^{-3}, $E_{Ts} = 0.4$ eV, $\sigma_{ns} = 5 \times 10^{-14}$ cm^2. Data from [8].

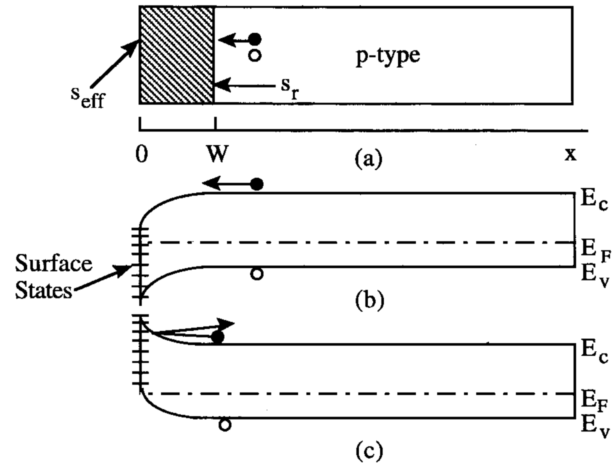

Fig. 9. Cross section and band diagram for a p-type sample with (a) and (b) depleted surface, and (c) accumulated surface.

were chosen to correspond to those in Fig. 5. The more realistic cross sections for SiO_2/Si interfaces are those in Fig. 8.

A surface is usually specified in terms of its surface recombination velocity s_r. The question is, where in the sample is this velocity specified? It is usually assumed that s_r refers to the surface. That is not necessarily true. Consider the p-type wafer with a surface-induced space-charge region in Fig. 9(a) and (b). Suppose excess electron-hole pairs are generated in the neutral region of the sample and let us consider those minority electrons that diffuse toward the surface, indicated by the electron with the arrow. Electrons that make it to the edge of the scr at $x = W$ will drift across the scr to recombine at the surface. They do not recombine at $x = W$. Surface recombination obviously occurs at the surface, neglecting bulk and scr recombination. However, equations describing the behavior of minority carriers are derived with a surface recombination velocity boundary condition s_r at $x = W$ *not* at $x = 0$. The actual surface recombination velocity is s_{eff}. Both s_r and s_{eff} are proportional to the density of surface states or interface traps. Hence, a measure of s_{eff} is a measure of s_r, but the two are rarely identical.

We see then, that surface recombination is a more complicated process than bulk recombination, because it depends not only on the density of surface states or interface traps, but also on the state of the surface [9]. Is the surface accumulated, depleted, or inverted? This would depend, for example, on the charge state of surface states, i.e., are they positively or negatively charged. Do they, therefore, induce a depleted or accumulated surface? For example, a surface might be depleted, as in Fig. 9(a) and (b), and present an attractive potential to minority carriers. With increased injection level, which may be the result of increased light intensity in a PCD measurement, the surface potential approaches zero and the surface-induced space-charge region vanishes [10]. Consequently, the attractive potential for minority carriers also vanishes and surface recombination diminishes, as illustrated in Fig. 8. Accumulated surfaces, shown in Fig. 9(c), present a repulsive potential to minority carriers with a concomitant low surface recombination velocity. It is for this reason that high/low p^+/p surfaces are used when low surface recombination is desired, e.g., at the rear surface of solar cells. This repulsive barrier diminishes with increasing injection level and surface recombination increases. Such considerations do not apply to bulk recombination, for the bulk potential is determined by doping density and injection level, but not by depletion or accumulation considerations.

III. Generation Lifetime

A. Shockley–Read–Hall Generation Lifetime

Each of the recombination processes of Fig. 2 has a generation counterpart. Optical ehp generation is the counterpart of radiative recombination and impact ionization is that of Auger recombination. The inverse of multiphonon recombination is thermal ehp generation characterized by the generation lifetime [4]

$$\tau_g = \tau_p e^{(E_T - E_i)/kT} + \tau_n e^{-(E_T - E_i)/kT}. \tag{11}$$

τ_g is due to SRH generation and is the only generation lifetime usually considered, provided optical and impact ionization generation is negligible. Hence, we designate it simply as τ_g, *not* $\tau_{g,\text{SRH}}$. It is the time to generate one ehp thermally, and depends inversely on the impurity density and the capture cross section for electrons and holes, just as τ_r does. In addition, however, it depends exponentially on the energy level E_T as illustrated in Fig. 10. Comparison of the curves in Fig. 10 with those in Fig. 5 show τ_g to be much more sensitive to E_T and capture cross section than τ_{SRH}, because ehp generation, being a thermally activated process, is very sensitive to the impurity energy level. Recombination, on the other hand, is relatively insensitive to E_T, at least over the central portion of the bandgap, as illustrated in Fig. 5.

The generation lifetime can be quite large if E_T does not coincide with E_i as shown in Fig. 10. τ_g is sometimes written as

$$\tau_g \approx \tau_r e^{|E_T - E_i|/kT} \tag{12}$$

if τ_r is the SRH recombination lifetime. Generally, τ_g is higher than τ_r, with typically $\tau_g \approx$ (50–100)τ_r, at least for Si devices, where detailed comparisons have been made [4].

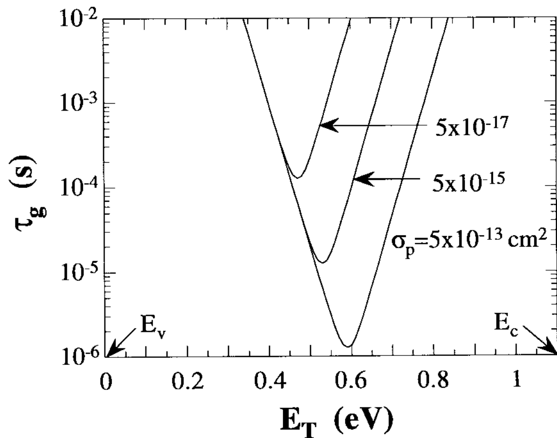

Fig. 10. τ_g versus E_T for $N_T = 10^{12}$ cm^{-3}, $\sigma_n = 5 \times 10^{-14}$ cm^2.

Figs. 5 and 10 show clearly that τ_g and τ_r can be very different, even for the same impurity and show that the measurement technique plays an important role when measuring the lifetime. A measurement technique that determines the recombination lifetime, such as photoconductance decay or surface photovoltage, will give a very different answer than the generation lifetime measured, for example, by the pulsed MOS capacitor method. This is effectively illustrated in Fig. 11 where both $\tau_{g,\text{eff}}$ and $\tau_{r,\text{eff}}$ are shown for Fe-contaminated Si. The effective lifetimes are defined later. Although there is a fair amount of scatter in the data, $\tau_{g,\text{eff}}$ is clearly higher than $\tau_{r,\text{eff}}$. It is important, obviously, to specify the measurement method as these figures illustrate. This, however, is not always done. Furthermore, the generation lifetime is sometimes referred to as the minority carrier generation lifetime, creating further confusion. Recall that in the space-charge region of a reverse-biased device one cannot speak of a minority carrier lifetime.

B. Shockley–Read–Hall Surface Generation Velocity

The *surface generation velocity* s_g is given by [5]

$$s_g = \frac{s_n s_p}{s_n e^{(E_{it}-E_i)/kT} + s_p e^{-(E_{it}-E_i)/kT}}. \tag{13}$$

It can be thought of as that velocity with which carriers, generated at the surface or interface, leave that surface. s_g is proportional to the surface or interface state density through s_n and s_p, defined in (10). In contrast to bulk deep-level impurities that have discrete energy levels in the bandgap, interface traps or surface states are distributed in energy throughout the semiconductor bandgap. Furthermore, the density of interface traps usually varies through the bandgap, further complicating the analysis and not considered here. Another consideration is the state of the surface. Generation is highest for a depleted surface and diminishes for both accumulated and inverted surfaces. This is most elegantly illustrated with leakage current measurements of gate-controlled diodes. In this test structure the semiconductor surface, controlled by a gate, can be accumulated, depleted, or inverted and the resultant leakage current depends very sensitively on the state of that surface [11]. Again, the type of recombination/generation velocity that is determined depends very much on the measurement technique.

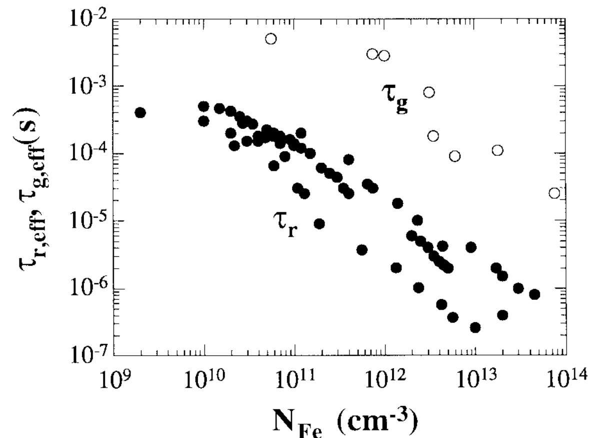

Fig. 11. τ_g and τ_r versus Fe density. For sources of experimental data see Figs. 12 and 18.

In general, $s_g < s_r$. For example, $s_g \approx 0.1$–1 cm/s for well passivated SiO_2/Si interfaces, whereas s_r can be 100–1000 cm/s for that same interface. Of course, s_r also depends on injection level.

IV. Effective Lifetimes

A. Recombination Lifetime/Surface Recombination Velocity

The bulk recombination lifetime itself is independent of surface recombination. However, the measured recombination lifetime, frequently referred to as the effective recombination lifetime $\tau_{r,\text{eff}}$, is dependent on surface recombination as carriers recombine both in the bulk as well as at the surface. $\tau_{r,\text{eff}}$ can be expressed as [5]

$$\tau_{r,\text{eff}} = \left(\frac{1}{\tau_r} + \frac{1}{\tau_s}\right)^{-1} = \frac{\tau_r}{1 + \tau_r/\tau_s} \tag{14}$$

where τ_s, the surface lifetime, is given by

$$\tau_s = \frac{1}{\beta^2 D_n}. \tag{15}$$

D_n is the electron diffusion constant and β is obtained from a solution of the equation [12]

$$\tan\left(\frac{\beta t}{2}\right) = \frac{s_r}{\beta D_n} \tag{16}$$

where t is the sample thickness. In the limits of low or high surface recombination velocity s_r, the surface lifetime becomes

$$\tau_s(s \to 0) = \frac{t}{2 s_r}; \quad \tau_s(s \to \infty) = \frac{t^2}{\pi^2 D_n}. \tag{17}$$

Equation (14) is plotted in Fig. 12 as a function of impurity density. For impurity densities below about 10^{12} cm^{-3}, s_r must be very low to be able to measure the true recombination lifetime. If that is not the case, then the effective lifetime can be much lower than the bulk lifetime. Also shown on Fig. 12 are experimental data for Fe-contaminated Si. Although there is a fair amount of scatter in the data, the general trend is that predicted by theory. The effective lifetime is inversely

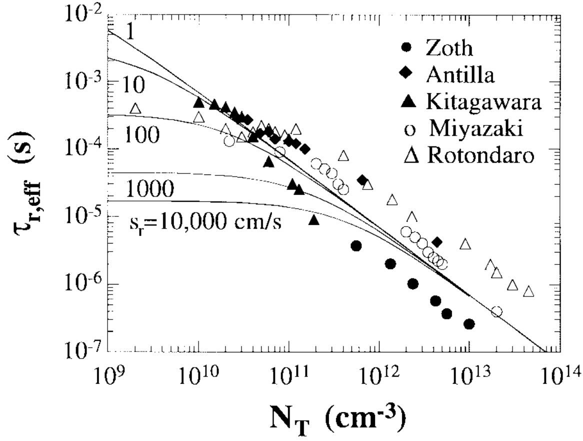

Fig. 12. $\tau_{r,\text{eff}}$ versus N_T for $E_T = 0.4$ eV, $p_o = 10^{15}$ cm^{-3}, $\sigma_n = 2 \times 10^{-14}$ cm^2, $\sigma_p = 5 \times 10^{-16}$ cm^2, $\eta = 0.01$, $t = 650$ μm, $T = 300$ K. The experimental data sources are for Fe in Si.

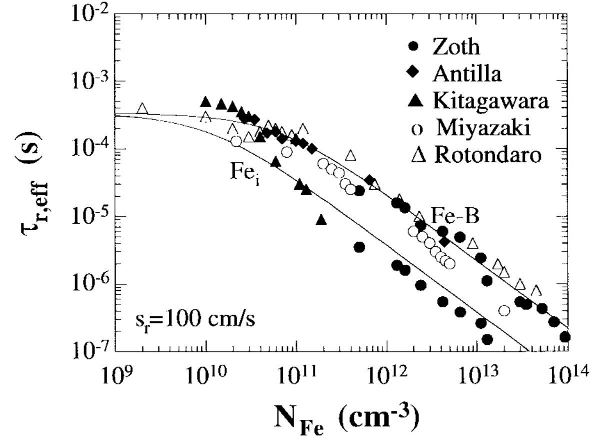

Fig. 13. $\tau_{r,\text{eff}}$ versus N_{Fe} for $p_o = 10^{15}$ cm^{-3}, $\sigma_p = 5 \times 10^{-16}$ cm^2, $\eta = 0.01$, $t = 650$ μm, $T = 300$ K.

proportional to impurity density only in that range where the bulk lifetime dominates the surface lifetime, i.e., at the higher impurity densities. For low impurity densities, $\tau_{r,\text{eff}}$ becomes independent of N_T and is governed chiefly by s_r.

The scatter in the experimental data is caused by Fe being in one of two states in p-Si: either interstitial iron (Fe_i) or iron-boron pairs (Fe-B). When an Fe-contaminated, B-doped Si wafer has been at room temperature for a few hours, the iron forms pairs with boron. Upon heating at around 200 °C for a few minutes or illuminating the device, the Fe-B pairs dissociate into interstitial Fe and substitutional B. The recombination properties of Fe_i differ from those of Fe-B. Fig. 13 shows the effective lifetime for these two states of Fe in B-doped Si using the recombination coefficients of Zoth and Bergholz [13]. The ratio $\tau_{r,\text{eff}}(\text{Fe-B})/\tau_{r,\text{eff}}(\text{Fe}_i) \approx 10$ and the data points agree quite well with theory. It is this ratio, or more commonly the ratio of minority carrier diffusion lengths, that is commonly used to determine the Fe contamination in B-doped Si. By measuring the diffusion length of an Fe-contaminated sample before (L_i) and after (L_f) Fe-B pair dissociation, N_{Fe} is [13]

$$N_{\text{Fe}} = 1.05 \times 10^{16} \left(\frac{1}{L_f^2} - \frac{1}{L_i^2} \right) \text{cm}^{-3} \tag{18}$$

with diffusion lengths in units of μm. Similar to iron, chromium in B-doped Si also forms pairs. However, in this case the diffusion length increases after pair dissociation and the appropriate relationship is [14]

$$N_{\text{Cr}} = 10^{16} \left(\frac{1}{L_i^2} - \frac{1}{L_f^2} \right) \text{cm}^{-3}. \tag{19}$$

To separate bulk and surface lifetimes, one can use the approximation of (17) in (14) and vary the sample thickness t. For low s_r one plots $1/\tau_{r,\text{eff}}$ versus $1/t$. The intercept of such a plot yields τ_r and the slope yields s_r as shown in Fig. 14(a). For high s_r, usually obtained by sandblasting the sample surfaces, one plots $1/\tau_{r,\text{eff}}$ versus $1/t^2$. The intercept of this plot yields τ_r and the slope yields D_n as shown in Fig. 14(b).

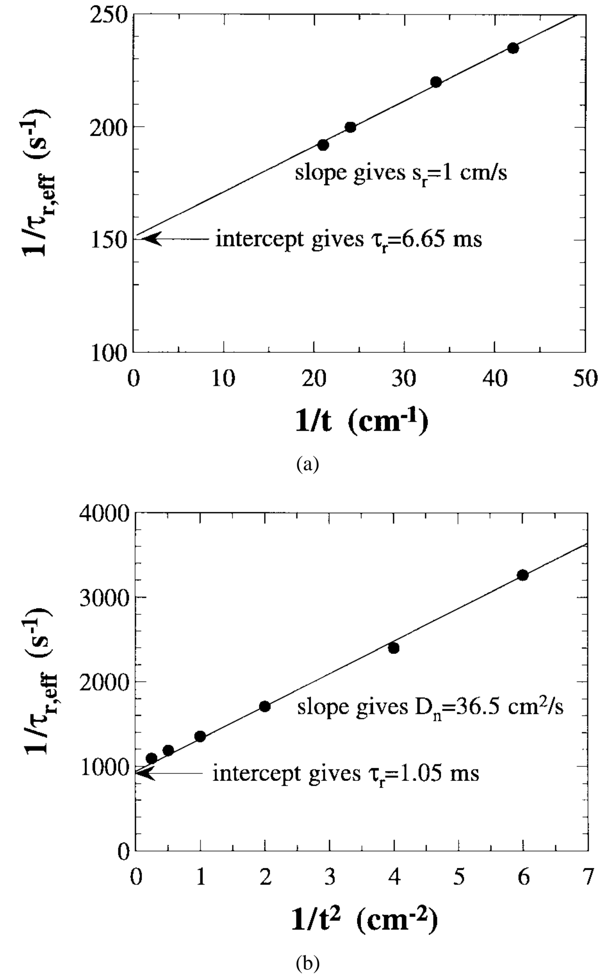

Fig. 14. (a) $1/\tau_{r,\text{eff}}$ versus $1/t$ to extract τ_r and s_r. After [19]; (b) $1/\tau_{r,\text{eff}}$ versus $1/t^2$ to extract τ_r and D_n; p-Si, 18.3 Ω·cm. After [20].

Low surface recombination velocities can be achieved by treating the surface in one of several ways. Oxidized Si surfaces have been reported with $s_r \approx 20$ cm/s, [21] but values

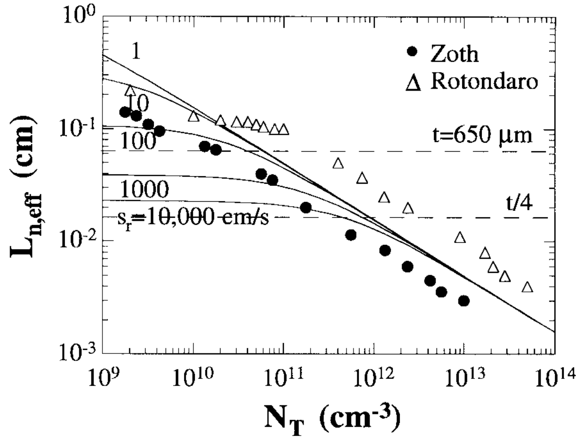

Fig. 15. $L_{n,\text{eff}}$ versus N_T for $E_T = 0.4$ eV, $p_o = 10^{15}$ cm^{-3}, $\sigma_n = 2 \times 10^{-14}$ cm^2, $\sigma_p = 5 \times 10^{-16}$ cm^2, $\eta = 0.01$, $t = 650$ μm, $T = 300$ K. The experimental data sources are shown on the figure.

as low as 1 cm/s have been observed [19]. Immersing a bare Si sample in one of several solutions can reduce s_r even below this value. For example, immersion in HF has given $s_r = 0.25$ cm/s [22]. Immersing the sample in iodine in methanol has given $s_r \approx 4$ cm/s [23]. In a series of experiments, a float-zone Si sample was immersed in concentrated HF, then removed and the $\tau_{r,\text{eff}}$ was measured as a function of time. Subsequently the sample was immersed in an iodine-saturated ethanol solution, removed and then measured. The values of s_r in air following the removal of the sample from either solution were $s_r \approx 998$ cm/s for the HF-passivated surface and $s_r = 394$ cm/s for the iodine-passivated surface [24].

The *minority carrier diffusion length* L_n is, of course, also affected by surface recombination. We show in Fig. 15 a plot of $L_{n,\text{eff}}[L_{n,\text{eff}} = (\tau_{r,\text{eff}} D_n)^{1/2}]$ versus N_T as a function of s_r similar to the plot of Fig. 12. Also shown in Fig. 15 is the thickness $t = 650$ μm used in the calculation of (14). In diffusion length measurements by techniques like surface photovoltage, it is usually assumed that the longest diffusion length that can be reliably measured for a wafer of thickness t is $L_{n,\text{eff}} = t/4$. This line is also indicated on Fig. 15. The experimental data points for Fe in Si in Fig. 15 give reasonably good agreement with the calculations. We have again the question of the state of the Fe, i.e., Fe_i or Fe-B.

The sample needs to be fairly thick to obtain the true recombination lifetime or true minority carrier diffusion length, especially for samples with low impurity densities. This is illustrated in Fig. 16, where both $\tau_{r,\text{eff}}$ and $L_{n,\text{eff}}$ are shown as a function of sample thickness. Note that the usual assumption of $t \geq 4L_n$ is observed. In fact the sample needs to be on the order of 0.3-cm thick to reach true τ_r and L_n for this example. Certainly, if the sample is thinner than $4L_n$, special precautions must be followed to extract the true lifetime or diffusion length from the experimental data. This is possible to do, but not routinely used. It was recently shown that diffusion lengths exceeding the sample thickness by as much as a factor of 2.5 can be extracted with the appropriate analysis [25]. If such analyzes are not used, then erroneous lifetimes or diffusion lengths may be obtained. This point of sample thickness, surface recombination velocity, and comparison between PCD and SPV was recently addressed. Lifetimes determined by these two techniques agree, provided the experimental data are properly analyzed. Examples of such correlation are shown in Fig. 17, with diffusion length data obtained from SPV measurements converted to lifetimes [18], [26].

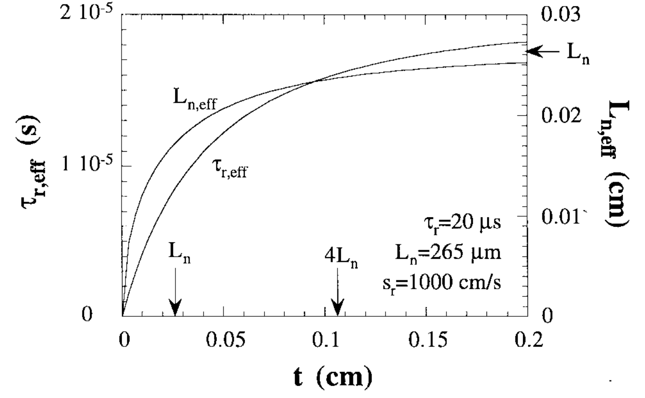

Fig. 16. $\tau_{r,\text{eff}}$ and $L_{n,\text{eff}}$ versus t for $\tau_r = 20$ μs, $L_n = 265$ μm, and $s_r = 1000$ cm/s.

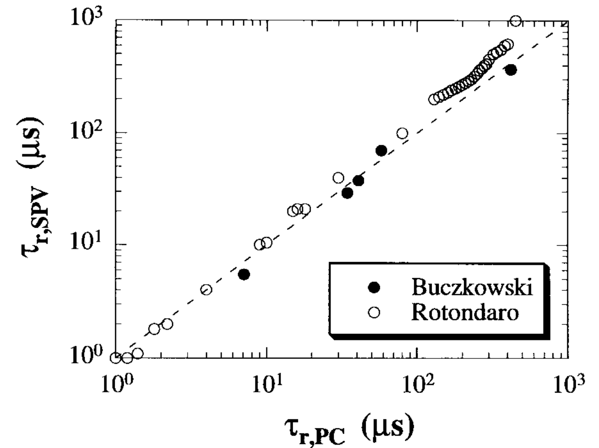

Fig. 17. $\tau_{r,\text{eff}}$ determined from photoconductance decay and surface photovoltage measurements. Data after [18] and [26].

B. Generation Lifetime/Surface Generation Velocity

Generation lifetime measurements are usually made with a pulsed MOS capacitor (MOS-C) or a reverse biased pn junction. The various generation mechanisms of a reverse-biased junction are shown in Fig. 18. They are similar in an MOS-C. Generation rate is 1) due to R–G centers in the scr; 2) due to interface traps at the SiO_2/Si interface; 3) due to R–G centers in the quasineutral bulk; and 4) due to the back surface. The generation rate for the various mechanisms can be written as [27]

$$G = \frac{qn_i W A_J}{\tau_g} + qn_i s_g A_S + \frac{qn_i^2 D_n A_J}{N_A L_{n,\text{eff}}} \tag{20}$$

where the diffusion length $L_{n,\text{eff}}$ is an effective diffusion length that couples the bulk diffusion length L_n [mechanism (3)] with the surface generation velocity at the back surface

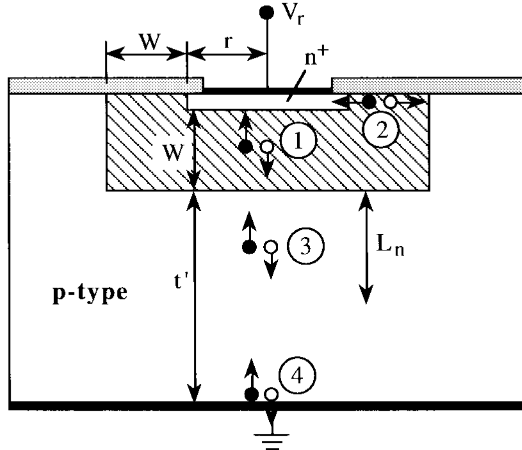

Fig. 18. Generation mechanisms in a reverse-biased np junction.

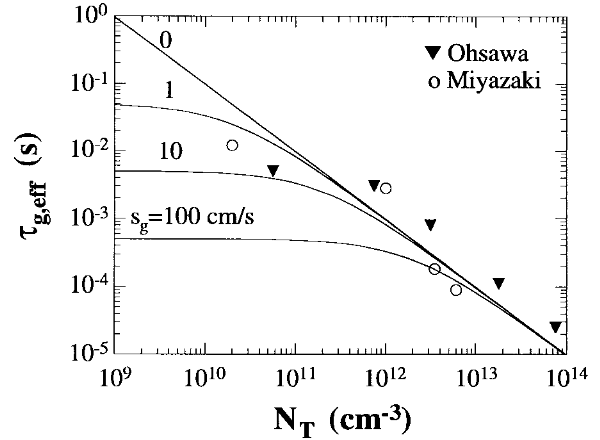

Fig. 19. $\tau_{g,\text{eff}}$ versus N_T for $E_T = 0.4$ eV, $\sigma_n = 5 \times 10^{-14}$ cm^2, $\sigma_p = 5 \times 10^{-16}$ cm$^2, r = 1$ mm.

s_c [mechanism (4)] through the relationship

$$L_{n,\text{eff}} = L_n \frac{\cosh(\zeta) + (s_c L_n/D_n)\sinh(\zeta)}{(s_c L_n/D_n)\cosh(\zeta) + \sinh(\zeta)} \tag{21}$$

where $\zeta = t'/L_n$. For simplicity we assume the scr width at the surface W to be identical to that in the bulk, both shown as W in Fig. 18. This assumption gives the surface area as $A_S = 2\pi r W$ and the junction area as $A_J = \pi r^2$, where r is the radius of a circular diode. Then (20) becomes

$$G = \frac{qn_i W A_J}{\tau_{g,\text{eff}}} + \frac{qn_i^2 D_n A_J}{N_A L_{n,\text{eff}}} \tag{22}$$

where the effective generation lifetime $t_{g,\text{eff}}$, given by

$$\tau_{g,\text{eff}} = \frac{\tau_g}{1 + \tau_g/\tau_s} \tag{23}$$

is a combination of space-charge region bulk and surface generation, with τ_s the surface generation lifetime, related to the surface generation velocity s_g by the expression

$$\tau_s = \frac{r}{2s_g}. \tag{24}$$

Equation (24) follows directly from (20) using the expressions for A_S and A_J.

C. What Actually Measured?

Just as surfaces or interfaces play an important role during recombination lifetime measurements, so they do during generation lifetime measurements as well. The effect of surface generation is illustrated in Fig. 19, where $\tau_{g,\text{eff}}$ is plotted versus N_T as a function of s_g. For well-passivated surfaces, $s_g \leq 1$ cm/s and $\tau_{g,\text{eff}}$ measurements give true τ_g values for impurity densities as low as $\sim 10^{11}$ cm^{-3} for the parameters chosen for Fig. 19.

So far we have considered scr generation, assuming quasineutral region (qnr) generation to be negligible. It is generally found that for Si at room temperature, scr generation dominates qnr generation. When that is not true, a further complication arises in the interpretation of generation lifetime measurements. When might that happen? Inspection of the qnr generation term in (22) shows it to be proportional to $n_i^2/L_{n,\text{eff}}$. This term increases with increasing temperature due to n_i^2 and when $L_{n,\text{eff}}$ decreases. For today's Si devices, qnr generation dominates over scr generation typically for temperatures higher than 50–70 °C due to the n_i^2 term, even if the impurity density is uniform throughout the entire sample [27].

However, even at room temperature it is possible for the qnr term not to be negligible when, for example, $L_{n,\text{eff}}$ decreases. This can occur in devices in which oxygen precipitation in the wafer interior causes significant diffusion length reduction, still maintaining high $\tau_{g,\text{eff}}$ in the scr of the surface denuded zone [28]. Fortunately, it is relatively simple to separate scr from qnr generation terms. Plotting the generation rate G as a function of W gives a plot with slope $qn_i A_J/\tau_{g,\text{eff}}$ and intercept $qn_i^2 D_n A_J/N_A L_{n,\text{eff}}$, allowing $\tau_{g,\text{eff}}$ to be determined from the slope and $L_{n,\text{eff}}$ from the intercept.

An example of recombination lifetime reduction due to oxygen precipitation is shown in Fig. 20. In this sample, a surface denuded zone (DZ) about 20-μm wide was formed by oxygen outdiffusion. Then τ_r and τ_g were measured, before any precipitation, with $\tau_g/\tau_r \approx 100$, as is usual for Si. Then the wafer was annealed to cause oxygen precipitation in the interior, leaving the denuded zone without precipitates because the oxygen density is too low for precipitation there. The lifetimes were remeasured and now $\tau_g/\tau_r \approx 50\,000$ [28]. Not only did τ_r decrease due to precipitation as expected, but τ_g increased due to internal gettering of metallic impurities from the DZ. Clearly very different regions in the wafer are characterized during these two measurements. This example exhibits very clearly how the measurement of τ_g and τ_r is very powerful in elucidating the recombination/generation properties. It also shows the different regions that are sampled during the measurement. The generation lifetime measurement samples the wafer over a space-charge region width, controlled by the gate voltage applied to an MOS capacitor. The recombination lifetime, however, samples a depth of approximately the minority carrier diffusion length, which is not under the experimenter's control, once the sample is made.

Other examples of local lifetime variations along the *wafer thickness* direction, include epitaxial layers grown on highly

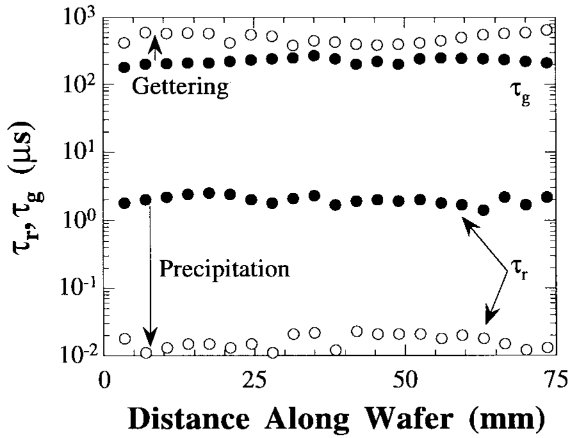

Fig. 20. Recombination/generation lifetimes before and after oxygen precipitation. Data from [28].

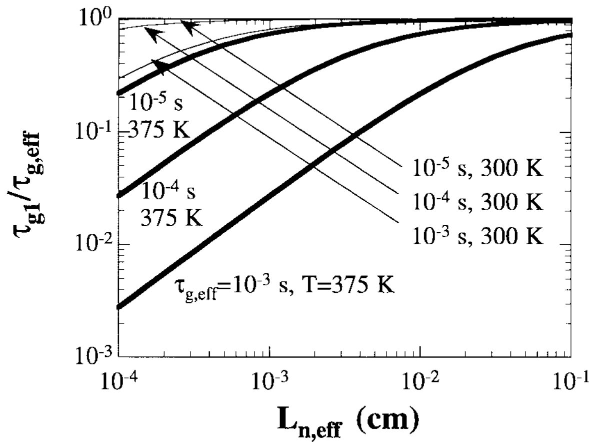

Fig. 21. Normalized τ_{g1} versus $L_{n,\mathrm{eff}}$ as a function of $\tau_{g,\mathrm{eff}}$. Si with $D_n = 35$ cm$^2/s, N_A = 10^{16}$ cm$^{-3}, W = 2$ μm.

doped substrates and silicon-on-insulator (SOI). In either case, the layer thickness is much less than the diffusion length. There are equations to interpret recombination lifetime and diffusion length measurements for such cases [29], but the interpretation is difficult as surface and interface recombination as well as varying lifetimes in the two regions of the epi case, play significant roles. The generation lifetime, however, is a suitable measurement parameter in these cases, since the sampling depth is the scr width. For example, the only method that gives useful R–G information for SOI wafers with Si layer thicknesses on the order of 0.1 μm, is the τ_g measurement [31].

If we measure a device parameter that depends on the generation rate, such as the pn junction leakage current, then all generation mechanisms must be considered. To see this, let us write (22) as [29]

$$G = \frac{qn_i W A_J}{\tau_{g1}} \tag{25}$$

where

$$\tau_{g1} = \tau_{g,\mathrm{eff}} \left(1 + \frac{n_i D_n \tau_{g,\mathrm{eff}}}{N_A W L_{n,\mathrm{eff}}}\right)^{-1}. \tag{26}$$

To illustrate this effect, we have plotted $\tau_{g1}/\tau_{g,\mathrm{eff}}$ versus $L_{n,\mathrm{eff}}$ as a function of $\tau_{g,\mathrm{eff}}$ and temperature in Fig. 21. For room temperature, qnr generation plays a minor role in this example, even for very short $L_{n,\mathrm{eff}}$. However, for elevated temperatures, the effect is quite pronounced, largely due to the ni term in (26).

V. Summary

We have tried to shed some light on "lifetimes in semiconductors," a topic that has caused much confusion over the years. To this end we have taken first-order concepts and equations and illustrated them with appropriate figures. This is perhaps an opportune time to discuss this topic since lifetime, which has largely been ignored by the IC community in the past, is emerging as an important parameter describing material, process, and equipment cleanliness.

The bulk of a sample is characterized by:

- recombination lifetime;
- generation lifetime.

Recombination lifetime is the result of one or more of three recombination mechanisms:

- Shockley–Read–Hall or multiphonon recombination;
- radiative recombination;
- Auger recombination.

The surface or interface of a sample is characterized by:

- surface recombination velocity;
- surface generation velocity.

Recombination/generation lifetime and surface recombination/generation velocity depend on:

- injection level;
- energy of the recombination center;
- R–G center capture cross sections;
- temperature.

What is actually measured is always a mixture of bulk and surface recombination or generation. Which of these dominates depends on such factors as sample geometry, recombination/generation lifetime, and surface recombination/generation velocity. One aspect of lifetime measurements that is often overlooked is the volume that is sampled during the measurement. For τ_r measurements the volume is proportional to the minority carrier diffusion length, which can be hundreds of microns. For τ_g measurements it is the space-charge region width, which is typically a micron or less. This can have important implications when one is dealing with thin semiconductor layers, e.g., epitaxial layers and silicon-on-insulator. With all of these considerations, it is not surprising so much has been written about lifetime, and that such confusion and so many lifetime values exist.

Acknowledgment

Many of these concepts were developed over a number of years and the author thanks colleagues for many discussions, and students for some of the measurements. He also thanks H. Huff for encouragement to put these thoughts to paper.

References

[1] R. N. Hall, "Electron-hole recombination in germanium," *Phys. Rev.*, vol. 87, p. 387, July 1952.

[2] W. Shockley and W. T. Read, "Statistics of the recombinations of holes and electrons," *Phys. Rev.*, vol. 87, pp. 835–842, Sept. 1952.

[3] R. N. Hall, "Recombination processes in semiconductors," *Proc. IEE* vol. 106B, pp. 923–931, Mar. 1960.
[4] D. K. Schroder, "The concept of generation and recombination lifetimes in semiconductors," *IEEE Trans. Electron Devices*, vol. ED-29, pp. 1336–1338, Aug. 1982.
[5] ——, *Semiconductor Material and Device Characterization.* New York: Wiley, 1990, ch. 8.
[6] S. K. Pang and A. Rohatgi, "Record high recombination lifetime in oxidized magnetic Czochralski silicon," *Appl. Phys. Lett.*, vol. 59, pp. 195–197, July 1991.
[7] J. Cornu, R. Sittig, and W. Zimmermann, "Analysis and measurement of carrier lifetimes in the various operating modes of power devices," *Solid-State Electron.*, vol. 17, pp. 1099–1106, Oct. 1974.
[8] A. G. Aberle, S. Glunz, and W. Warta, "Impact of illumination level and oxide parameters on Shockley–Read–Hall recombination at the Si-SiO_2 interface," *J. Appl. Phys.*, vol. 71, pp. 4422–4431, May 1992; S. J. Robinson, S. R. Wenham, P. P. Altermatt, A. G. Aberle, G. Heiser, and M. A. Green, "Recombination rate saturation mechanisms at oxidized surfaces of high-efficiency silicon solar cells," *J. Appl. Phys.*, vol. 78, pp. 4740–4754, Oct. 1995.
[9] T. Otaredian, "The influence of the surface and oxide charge on the surface recombination process," *Solid-State Electron.*, vol. 36, pp. 905–915, June 1993.
[10] E. O. Johnson, "Large-signal surface photovoltage studies with germanium," *Phys. Rev.*, vol. 111, pp. 153–166, July 1958.
[11] D. J. Fitzgerald and A. S. Grove, "Surface recombination in semiconductors," *Surf. Sci.*, vol. 9, pp. 347–369, Feb. 1968.
[12] K. L. Luke and L. J. Cheng, "Analysis of the interaction of a laser pulse with a silicon wafer: determination of bulk lifetime and surface recombination velocity," *J. Appl. Phys.,* vol. 61, pp. 2282–2293, Mar. 1987.
[13] G. Zoth and W. Bergholz, "A fast, preparation-free method to detect iron in silicon," *J. Appl. Phys.*, vol. 67, pp. 6764–6771, June 1990.
[14] K. Mishra and R. Falster, Abstr. 426, Electrochem. Soc. Mtg. Extend. Abstr. 92-2, Toronto, Ont, Canada, Oct. 11–16, 1992, p. 632.
[15] O. J. Antilla and M. V. Tilli, "Metal contamination removal on silicon wafers using dilute acidic solutions," *J. Electrochem. Soc.*, vol. 139, pp. 1751–1756, June 1992.
[16] Y. Kitagawara, T. Yoshida, T. Hamaguchi, and T. Takenaka, "Evaluation of oxygen-related carrier recombination centers in high-purity Czochralski-grown Si crystals by the bulk lifetime measurements," *J. Electrochem. Soc.*, vol. 142, pp. 3505–3509, Oct. 1995.
[17] M. Miyazaki, S. Miyazaki, T. Kitamura, T. Aoki, Y. Nakashima, M. Hourai, and T. Shigematsu, "Influence of Fe contamination in Czochralski-grown silicon single crystals on LSI-yield related crystal quality characteristics," *Jpn. J. Appl. Phys.*, vol. 34, pp. 409–413, Feb. 1995.
[18] A. L. P. Rotondero, T. Q. Hurd, A. Kaniara, J. Vanhellemont, E. Simoen, M. M. Heyns, and C. Claeys, "Impact of Fe and Cu contamination on the minority carrier lifetime of silicon substrates," *J. Electrochem. Soc.,* vol. 143, pp. 3014–3019, Sept. 1996.
[19] S. K. Pang and A. Rohatgi, "A new methodology for separating Shockley–Read–Hall lifetime and Auger recombination coefficients from the photoconductivity decay technique," *J. Appl. Phys.*, vol. 74, pp. 5554–5560, Nov. 1993.
[20] T. Maekawa and K. Fujiwara, "Measurable range of bulk carrier lifetime for a thick silicon wafer by induced eddy current method," *Jpn. J. Appl. Phys.*, vol. 35, pp. 3955–3964, Aug. 1995.
[21] E. Yablanovitch, R. M. Swanson, W. D. Eades, and B. R. Weinberger, "Electron-hole recombination at the Si-SiO_2 interface," *Appl. Phys. Lett.*, vol. 48, pp. 245–247, Jan. 1986.
[22] E. Yablanovitch, D. L. Allara, C. C, Chang, T. Gmitter, and T. B. Bright, "Unusually low surface-recombination velocity on silicon and germanium surfaces," *Phys. Rev. Lett.*, vol. 57, pp. 249–252, July 1986.
[23] H. M'saad, J. Michel, J. J. Lappe, and L. C. Kimerling, "Electronic passivation of silicon surfaces by halogens," *J. Electron. Mat.*, vol. 23, pp. 487–491, May 1994.
[24] H. M'saad, J. Michel, A. Reddy, and L. C. Kimerling, "Monitoring and optimization of silicon surface quality," *J. Electrochem. Soc.*, vol. 142, pp. 2833–2835, Aug. 1995.
[25] J. Lagowski, A. M. Kontkiewicz, L. Jastrzebski, and P. Edelman, "Method for the measurement of long minority carrier diffusion lengths exceeding wafer thickness," *Appl. Phys. Lett.*, vol. 63, pp. 2902–2904, Nov. 1993.
[26] A. Buczkowski, G. Rozgonyi, and F. Shimura, "Photoconductance minority carrier lifetime versus surface photovoltage diffusion length in silicon," *J. Electrochem. Soc.*, vol. 140, pp. 3240–3245, Nov. 1993.
[27] D. K. Schroder, J. D. Whitfield, and C. J. Varker, "Recombination lifetime using the pulsed MOS capacitor," *IEEE Trans. Electron Devices*, vol. ED-31, pp. 463–467, Apr. 1984.
[28] D. K. Schroder, J. M. Hwang, J. S. Kang, A. M. Goodman and B. L. Sopori, "Lifetime and recombination concepts for oxygen-precipitated silicon," in *VLSI Science and Technology/1985,* M. Bullis and S. Broydo, Eds. Pennington, NJ: Electrochemical Society, May 1985, pp. 419–428.
[29] D. K. Schroder, "Effective lifetimes in high-quality silicon devices," *Solid-State Electron.*, vol. 27, pp. 247–251, Mar. 1984.
[30] A. Ohsawa, K. Honda, R. Takizawa, T. Nakanishi, M. Aoki, and N. Toyokura, "Effects of impurities on microelectronic devices," in *Semiconductor Silicon 1990*, H. R. Huff, K. G. Barraclough, and J. I. Chikawa, Eds. Pennington, NJ: Electrochemical Society, 1990, pp. 601–613.
[31] D. E. Ioannou, S. Cristoloveanu, M. Mukherjee, and B. Mazhari, "Characterization of carrier generation in enhancement-mode SOI MOSFET's," *IEEE Electron Device Lett.*, vol. 11, pp. 409–411, Sept. 1990.

Dieter K. Schroder (S'61–M'67–SM'78–F'96) received the B.S. and M.S. degrees in 1962 and 1964, from McGill University, Montreal, P.Q., Canada, and the Ph.D. degree from the University of Illinois, Urbana-Champaign, in 1968.

In 1968, he joined the Westinghouse Research Labs, where he was engaged in reserach on various aspects of semiconductor devices, including MOS devices, imaging arrays, power devices, and magnetostatic waves. He spent a year at the Institute of Applied Solid State Physics, Germany, in 1978. In 1981, he joined the Center for Solid State Electronics Research, Arizona State University, Tempe. His current interests are semiconductor materials and devices, characerization, low-power electronics, and defects in semiconductors. He has written two books *Advanced MOS Devices* and *Semiconductor Material and Device Characterization*, (New York: Wiley, 1990) and has published over 100 papers.

Dr. Schroder was a Distinguished National Lecturer, IEEE Electron Devices Society, in 1993 and 1994.